Dynamic suspension performance of an ultra-compact 5-DOF controlled axial gap type self-bearing motor for use in pediatric ventricular assist devices

Masahiro Osa[1*], Toru Masuzawa[1], Toshihiro Yamashita[1] and Eisuke Tatsumi[2]

[1] Ibaraki University, Japan

[2] National Cerebral and Vascular Center Research Institute, Japan

Masahiro.osa.630@vc.ibaraki.ac.jp

Abstract

Research interest in miniaturization of magnetically suspended motor is increased to develop next generation ventricular assist devices (VADs) for pediatric heart disease treatment. In this study, an ultra-compact 5-degrees of freedom (DOF) controlled axial gap type self-bearing motor which employ double stator mechanism has been proposed. A six-slot and four-pole self-bearing motor which has 22 mm in diameter and 34 mm in height, and centrifugal pump was fabricated. This paper investigated pump characteristics, and then dynamic impeller suspension performance with frequency response evaluation. The developed maglev pump for pediatric VAD demonstrated non-contact pump drive producing flow rate of 0.5-3.0 L/min against head pressure of around 100 mmHg at rotating speed of 4000-5000 rpm. In addition, the maglev motor indicated sufficient bandwidth for impeller suspension control during pump drive.

1 Introduction

Mechanical circulatory support (MCS) technology is strongly required for treatment of severe heart disease pediatric patients due to the shortage of donor hearts. However, these pediatric patients have to depend on extracorporeal pulsatile blood pumps which have high risk of adverse events such as blood clotting and infection. One of the most significant reasons above is that there are no implantable compact rotary blood pumps due to technical difficulty for miniaturization of impeller suspension technique with high durability and blood compatibility. Our research group has

* Masterminded and created the first stable version of this document

developed an ultra-compact magnetically levitated pediatric ventricular assist device (VAD) with double stator axial gap permanent magnet synchronous motor. Maglev VADs have significant advantages such as high durability, higher speed operation, and low hemolysis as well as less thrombosis compared to conventional blood pumps which have mechanically contacting bearings for impeller suspension. In ultra-compact maglev systems, which tend to have deterioration of magnetic suspension force, a guaranty of impeller suspension stability of the blood pump over operating conditions is significantly important. Especially, evaluation of dynamic response of the magnetic suspension control system must be needed for maglev rotary VADs. In this study, magnetic suspension performance of the developed ultra-compact maglev motor for pediatric VADs was investigated.

2 Material and Methods

2.1 Overview of 5-DOF controlled axial gap type self-bearing motor and principles of magnetic suspension control and motor drive

The maglev pediatric VAD consists of two six-slot axial flux motor stators and a four-pole centrifugal impeller as shown in Fig. 1. The impeller is magnetically suspended between the stators that have an identical structure as shown in Fig. 2. Concentrated windings for both magnetic suspension and rotation are integrated and wound on each stator tooth. A double stator mechanism enhances rotating torque production and provides 5-DOF active control of impeller postures. An axial position (z) of the impeller is controlled with field strengthening and field weakening of impeller four-pole magnetic fields by d-axis current regulation as shown in Fig. 3. A rotating speed (ωz) is controlled with conventional q-axis current regulation. Inclination angles (θx, θy) and radial positions (x, y) of the levitated impeller are controlled by utilizing P±2 pole algorithm. Inclination torque and radial suspension force were numerically and experimentally found in a previous study. Both control principles for the inclination angle around y-axis and the radial position in x direction with the double stator mechanism are shown in Fig. 4. When the stators produce inclination torque which has same amplitude and direction, the inclination angle of the levitated impeller can be regulated without the radial suspension force. In contrast, the radial position of the impeller can be regulated with radial suspension force when the inclination torque produced by both stators is regulated in opposite direction. The inclination around x-axis and the radial position in y direction can be controlled in a similar manner. The inclination and radial position of the levitated impeller can be controlled independently with double stator mechanism by regulating magnitude and direction of excitation current supplied to the stators to generate the two-pole rotating magnetic field.

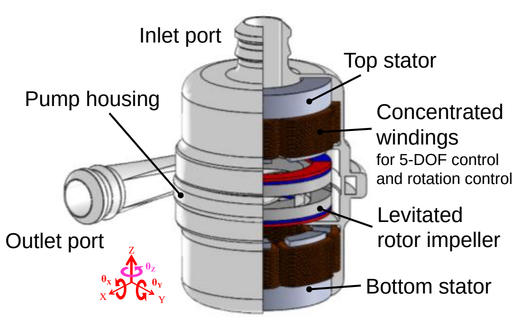

Figure 1: Schematic view of pediatric VAD with axial gap type self-bearing motor.

Figure 2: Developed ultra-compact double stator self-bearing motor.

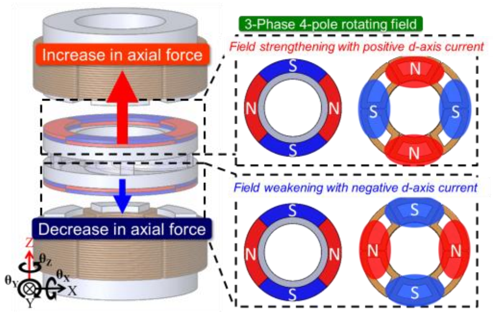

Figure 3: Axial position control with field strengthening and field weakening.

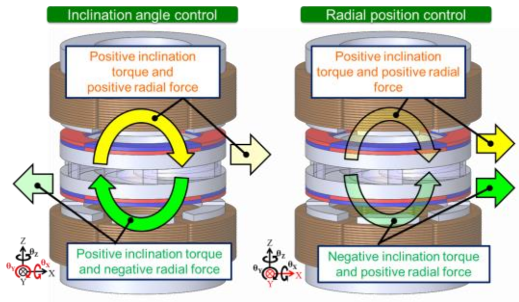

Figure 4: Inclination angle and radial position control with P+/- 2 pole algorithm.

2.2 Fabricated self-bearing motor for pediatric centrifugal VAD

Motor geometries listed in Table 1 were designed with 3D finite element method magnetic field analysis. A fabricated pediatric VAD with the 5-DOF controlled self-bearing motor are shown in Fig. 5. The motor is 22 mm in outer diameter and 34 mm in height. Sintered magnetic powder core (EU-69) is used for the motor stator core, and soft magnetic iron (SYU-1) is used for the rotor back iron. Neodymium permanent magnets have coercivity and residual flux density of 907 kA/m and 1.36 T. Concentrated copper windings of 123 turns are wound on each stator pole. The diameter of isolated copper wire is 0.3 mm. A double volute type centrifugal housing and six vanes closed impeller were designed with a computational fluid dynamics simulation. The inlet and outlet port diameter are 6 mm. The movable ranges of the impeller in axial direction, in radial direction and in inclination angle were set to +/-0.3 mm, +/-0.5 mm, and 1.4 degrees.

Table 1 Motor geometric parameters.

Inner diameter (mm)	16.8
Outer diameter (mm)	22
Pole height (mm)	9.3
Slot width (mm)	3.8
PM thickness (mm)	0.8
Rotor back iron thickness	2

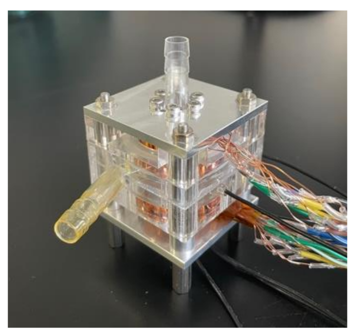

Figure 5: Developed centrifugal blood pump with axial gap self-bearing motor for pump testing.

2.3 Control system for magnetic suspension and rotation of 5-DOF controlled self-bearing motor

The developed rotary blood pump with the self-bearing motor was combined with a digital feedback control system. A schematic diagram of a 5-DOF PID control system is shown in Fig. 6. Digital PID controllers are implemented on a micro-processor board MicroLabBox (dSPACE GmbH,

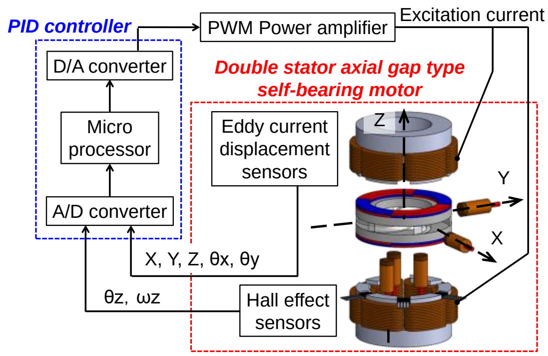

Figure 6: 5-DOF control and motor drive system with digital PID controller.

Table 2 PID control gains for rotor position regulation.

	P	I	D
Z	10 (A/mm)	0.05 (A/(mm・s))	0.002 (A s/mm)
θx, θy	1.5 (A/deg)	0 (A/(deg・s))	0.002 (A/(deg・s))
ωz	0.0005 (A/rpm)	0.0018 (A/(rpm・s))	—

Paderborn Germany) with MATLAB/Simlink for the active 5-DOF control of the impeller postures. Three eddy current displacement sensors (PU-03A, Applied Electronics Corporation) are located inner side of the stator poles to measure an axial position and inclination angles around x and y axes of the levitated impeller. Impeller radial positions in x and y direction are measured by other two eddy current displacement sensors located around outside of the levitated impeller. three Hall Effect sensors (Asahi KASEI Corporation) are placed on the stator slots to measure a rotating angle of the impeller with a sensitivity of 30 degrees electrical angle by detecting the magnetic flux produced by the rotor permanent magnets. The rotating speed is calculated by time derivative of the impeller rotating angle. Control current is calculated by PID controllers, and it is supplied by PWM power amplifier (JSP-090-10, Copley Controls) to the windings of the stators. Sampling and control frequency are 10 kHz. PID/PD gains were manually tuned to minimize the rotor vibration amplitude as listed on Table II.

2.4 Frequency response of magnetic suspension control system in self-bearing motor with 3-DOF control during pumping

5-DOF of impeller postures at different rotating speeds were evaluated to demonstrate a pump characteristic and non-contact impeller suspension during pump operation. Closed loop circulation circuit for pump drive testing is shown in Fig. 7. The levitated impeller was magnetically suspended and accelerated from 4000 rpm to 5000 rpm in water. After that, the frequency response of the axial position control system and the inclination control system was measured with a frequency sweeping

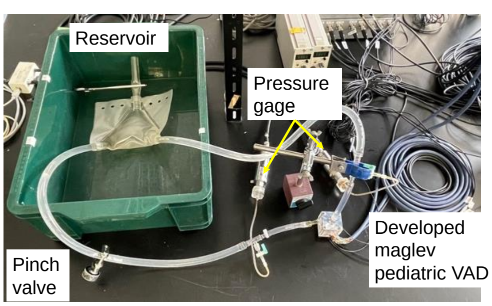

Figure 7: Experimental setup for pump testing and frequency response measurement.

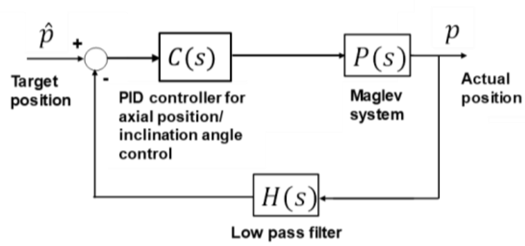

Figure 8: Block diagram for frequency response measurement.

method by using an FFT analyzer (DS-2100, DS-0264, Ono Sokki Corporation) at representative pump operating point of the speed of 4000 rpm and the flow rate of 1.5 L/min against the pressure head of around 90 mmHg for pediatric circulation. Amplitude of sinusoidal target signal which was determined as 0.1 mm in axial position and 0.1 degrees in inclination angle added to the control system as shown in Fig 8. The signal frequency was periodically varied from 10 Hz to 1 kHz. An input and an output are the target position and the actual levitated rotor displacement.

3 Results

Relationship between head pressure and flow rate produced by the developed maglev centrifugal blood pump is shown in Fig. 9. The developed pump produced the wide flow rate range of 0.5-3.0 L/min against the head pressure of 60-100 mmHg at the rotating speed of 4000-5000 rpm. The levitated impeller fully magnetically suspended at every operating condition. Mean oscillation amplitude in axial position, radial position and inclination angle were approximately 30 μm, 100 μm, 0.3 degrees, respectively. The oscillation was enough small to avoid mechanical contact between the levitated impeller and the pump housing. Bode diagram for the axial position control system and the inclination angle control system during pumping at rotating speed of 4000 rpm are shown in Fig. 10 and Fig. 11. Bandwidth in the axial position control system and the inclination control system were approximately 110 Hz and 50 Hz. In the inclination control system, the gain plots once increased around 60-150 Hz. However, this is not caused due to the inclination in response to input sinusoidal signal to the control system, and it should be excluded from the discussions.

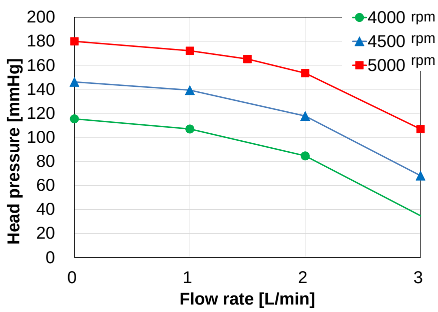

Figure 9: Pump characteristics of the developed maglev centrifugal blood pump.

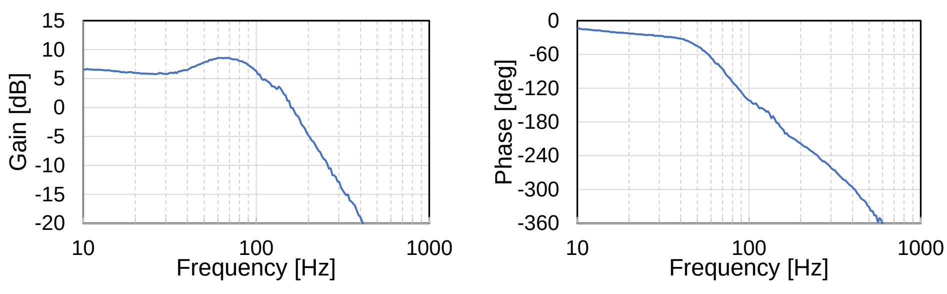

(a) Gain plot

(b) Phase plot

Figure 10: Bode diagram for axial position control system.

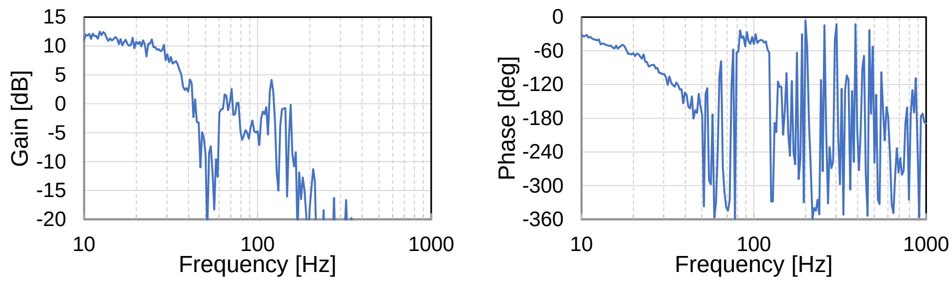

(a) Gain plot (b) Phase plot

Figure 11: Bode diagram for inclination angle control system.

4 Discussion

Magnetic suspension is one of the strongest candidates to achieve durable and biocompatible MCS devices. The developed ultra-compact self-bearing motor has a significantly contribute to progress of the VADs development for small pediatric patients. Investigation of the dynamic response in pump drive with the self-bearing motor is much important to indicate potential of the next generation maglev pediatric VADs. Sufficient pump performance with non-contact impeller suspension demonstrated that the developed pump will be available in pediatric circulation according to patients growing up. The magnetic suspension stability overall pump speeds would guarantee less hemolysis and anti-thrombogenicity. The wide bandwidth more than 100 Hz in axial position control system gives stable impeller suspension within the range of pump operating speed of 4000-5000 rpm (67-83 Hz). In contrast, although the inclination angle in pump testing was able to be sufficiently suppressed with active control, relatively small bandwidth of 50 Hz in the inclination control system was observed. This would be because that inclination stiffness produced by the active inclination control was little bit small, in addition, increase in damping effect in water. Further investigation of motor dynamic characteristics should be needed by carrying out a shaking test to completely demonstrate feasibility of the proposed self-bearing motor concept.

5 Conclusion

The ultra-compact double-stator axial gap type maglev motor with active 5-DOF control was developed. The developed pump demonstrated sufficient pump performance for the pediatric circulatory support. The feasibility of non-contact impeller suspension against the external disturbance in the maglev pediatric VAD operation was indicated by frequency response evaluation. A shaking test of the developed maglev pediatric VAD will be carried out to verify sufficient magnetic suspension stability with respect to external acceleration disturbance.

References

Baldwin, J.T.; Borovetz, H.S.; Duncan, B.W.; Gartner, M.J.; Jarvik, R.K.; Weiss, W.J.; Hoke, T.R. Weiss and Tracey R. Hoke. (2006), The National Heart, Lung, and Blood Institute Pediatric Circulatory Support. Circulation, 113, pp. 147–155.

Baldwin, J.T.; Borovetz, H.S.; Duncan, B.W.; Gartner, M.J.; Jarvik, R.K.; Weiss, W.J. (2011), The National, Heart, Lung, and Blood Instituted Pediatric Circulatolory Support Program: A Summary of the 5-year Experience. Circulation, 123, 1233–1240.

Miera, O.; Schmitt, K.R.; Delmo-Walter, E.; Ovroutski, S.; Hetzer, R.; Berger, F. (2014), Pump size of Berlin Heart EXCOR pediatric device influences clinical outcome in children. J. Heart Lung Trans., 33, pp. 816–821.

Lorts, A.; Zafar, F.; Adachi, I.; Morales, D.L. Morales. (2014), Mechanical Assist Devices in Neonates and Infants. Semin. Thoracic Cardiovasc. Surg. Pediatric Cardiac Surg. Annu. 17, pp. 91–95.

Gibber, M.; Wu, Z.J.; Chang, W.B.; Bianchi, G.; Hu, J.; Garcia, J.; Jarvik, R.; Griffith, B.P. (2010), In Vivo Experience of the Child-Size Pediatric Jarvik 2000 Heart: Update. Asaio J., 56, pp. 369–376.

Mehra, M.R.; Naka, Y.; Uriel, N.; Goldstein, D.J.; Cleveland Jr, J.C.; Colombo, P.C.; Walsh, M.N.; Milano, C.A.; Patel, C.B.; Jorde, U.P.; et al. (2017), A Fully Magnetically Levitated Circulatory Pump for Advanced Heart Failure. N. Engl. J. Med., 376, pp. 440–450.

Schoeb, R.; Barletta, N.; Fleischli, A.; Bourque, K.; Gernes, D.; Loree, H.; Richardson, J. S.; Poirier, V. (2000), Heartmate III: Bearingless Motor Design for A Malev Centrifugal LVAD. ASAIO Journal, 46, 191.

Wu, G.; Yang, L.; Li, H.; et al. (2019), Establishment of Ovine Model for CH-VAD Implantable Ventricular Assist Device. Journal of Mechanics in Medicine and Biology, 19, 1-10.

Emmanuel, S.; Watson, A.; Connellan, M.; et al. (2020), First in Man Anatomical Fitting Study of the BiVACOR Total Artificial Heart. The Journal of Heart and Lung Transplantation, 39, S189

Nicholas, A. G.; Daniel, L. T.; Nobuyuki, K.; Edward, W. P.; Toru, M. (2010), Axial Magnetic Bearing Development for the BiVACOR Rotary BiVAD/TAH. IEEE Trans. Biomed. Eng., 57, pp. 714-721.

Kurita, N.; Ishikawa, T.; Saito, N.; Masuzawa, T.; Daniel, L. T. (2018), A Double-Sided Stator Type Axial Bearingless Motor Development for Total Artificial Heart. IEEE Trans. Ind. Appl., 55, pp. 1516-1523.

Osa, M.; Masuzawa, T.; Tatsumi, E. (2012), 5-DOF Control Double Stator Motor for Paediatric Ventricular Assist Device. Proceedings of ISMB13; University of Virginia: Charlottesville, VA, USA.

Osa, M.; Masuzawa, T.; Orihara, R.; Tatsumi, E. (2019), Performance Enhancement of a Magnetic System in a Ultra Compact 5-DOF-Controlled Self-Bearing Motor for a Rotary Pediatric Ventricular-Assist Device to Diminish Energy Input. Actuators, 8, pp. 1-14.